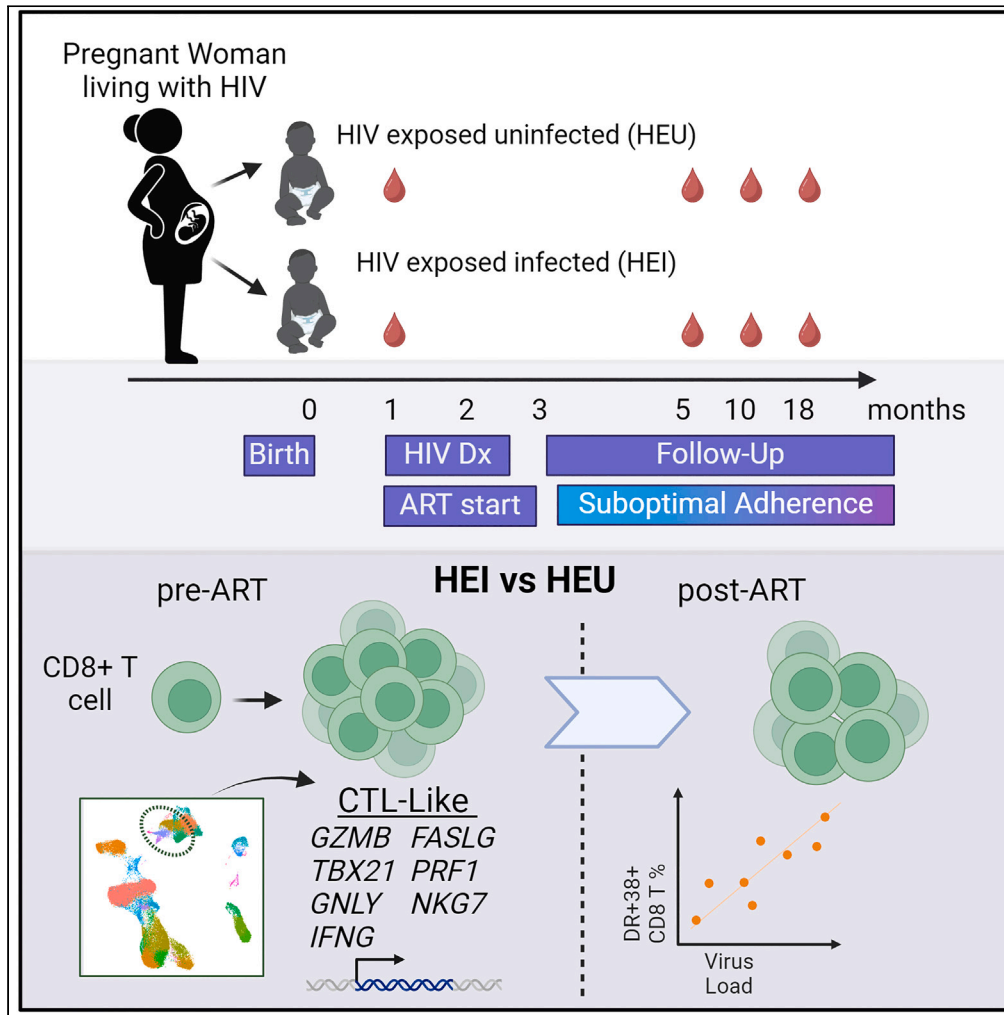**Article**

Accelerated CD8⁺ T cell maturation in infants with perinatal HIV infection

Lesley R. de Armas,
Vinh Dinh, Akshay
Iyer, ..., Paula Vaz,
Maria Grazia Lain,
Savita Pahwa

spahwa@med.miami.edu

Highlights

Effector: naive CD8 T cell ratios are elevated in infants with perinatal HIV

scRNA-seq revealed clonally expanded CTL-like cells in HEI prior to ART initiation

Correlates of pre-ART virus load include frequencies of circulating GC-like Tfh

CD38+HLADR+ CD8 T cells are strong correlate of virus load in perinatal HIV

Article

Accelerated CD8+ T cell maturation in infants with perinatal HIV infection

Lesley R. de Armas,[1,6] Vinh Dinh,[1,6] Akshay Iyer,[1] Suresh Pallikkuth,[1] Rajendra Pahwa,[1] Nicola Cotugno,[2,3] Stefano Rinaldi,[1] Paolo Palma,[2,3] Paula Vaz,[4] Maria Grazia Lain,[5] and Savita Pahwa[1,7,*]

SUMMARY

In perinatal HIV infection, early antiretroviral therapy (ART) initiation is recommended but questions remain regarding infant immune responses to HIV and its impact on immune development. Using single cell transcriptional and phenotypic analysis we evaluated the T cell compartment at pre-ART initiation of infants with perinatally acquired HIV from Maputo, Mozambique (Towards AIDS Remission Approaches cohort). CD8+ T cell maturation subsets exhibited altered distribution in HIV exposed infected (HEI) infants relative to HIV exposed uninfected infants with reduced naive, increased effectors, higher frequencies of activated T cells, and lower frequencies of cells with markers of self-renewal. Additionally, a cluster of CD8+ T cells identified in HEI displayed gene profiles consistent with cytotoxic T lymphocytes and showed evidence for hyper expansion. Longitudinal phenotypic analysis revealed accelerated maturation of CD8+ T cells was maintained in HEI despite viral control. The results point to an HIV-directed immune response that is likely to influence reservoir establishment.

INTRODUCTION

Advances in maternal antiretroviral therapy (ART) have dramatically reduced perinatal HIV transmission. However, more than 100,000 new vertical HIV infections occur annually, predominantly in Sub Saharan Africa, due to persistent challenges with access to continuous therapy and issues with disclosure and stigma.[1–4] Clinical trials (e.g., Children with HIV Early Antiretroviral Therapy (CHER), Child and Adolescent Reservoir Measurements on early suppressive ART (CARMA), and Early Infant Treatment (EIT)) in infants have shown the benefits of early treatment initiation (<12 weeks) in curtailing disease progression,[5–7] and the "Mississippi baby" demonstrated the possibility of prolonged albeit temporary ART-free remission with treatment initiation very early, within 30 h of birth.[8]

The role and nature of immune mechanisms that are important for HIV reservoir establishment and mechanisms of HIV persistence in children living with HIV on ART are poorly understood and may differ in infants compared to adults.[9–12] The immune system undergoes dynamic developmental changes from birth through infancy as it matures and acquires memory.[13,14] CD4+ and CD8+ T cells in the pre-term and neonatal periods exhibit a predominantly naive profile and develop a tolerogenic rather than inflammatory response characterized by differentiation of CD4+ T cells into T regulatory (FoxP3-expressing) cells.[15,16]

In this environment, in which the HIV reservoir is established, innate immune antiviral activity (e.g., natural killer [NK] cells) is considered to play a role in responding to HIV infection,[17] but these responses are also immature and tolerogenic compared to adults.[18,19] Infants are capable of mounting adaptive immune responses to HIV, but evolution of immune control mechanisms is unknown and likely to be influenced greatly by timing of ART initiation in perinatal HIV infection.[20] The magnitude of immune activation correlates with the HIV reservoir in adult HIV infections;[21] however, given the tolerogenic rather than pro-inflammatory bias in infants, it is not clear whether the same biomarkers will be as informative. Understanding the unique character of the neonatal adaptive immune system is therefore critical to guide the design of HIV cure strategies including immune-based interventions in early life.

In the current study, we assessed the composition of the T cell compartment in HIV exposed infected (HEI) infants at the time of ART initiation and longitudinally up to 18 months of age. Since maternal HIV infection has profound effects on pregnancy outcomes and infant development regardless of whether the infant acquires HIV during the perinatal period, we compared findings from HEI infants with age-matched HIV exposed uninfected (HEU) infants to determine independent biomarkers of age and plasma HIV RNA in infants.

[1]Department of Microbiology and Immunology, University of Miami Miller School of Medicine, Miami, FL, USA
[2]Research Unit of Clinical Immunology and Vaccinology, Bambino Gesù Children's Hospital, IRCCS, Rome, Italy
[3]Chair of Pediatrics, Department of Systems Medicine, University of Rome Tor Vergata, Rome, Italy
[4]Instituto Nacional de Saúde, Marracuene, Maputo Province, Mozambique
[5]Fundação Ariel Glaser contra o SIDA Pediátrico, Maputo, Mozambique
[6]These authors contributed equally
[7]Lead contact
*Correspondence: spahwa@med.miami.edu
https://doi.org/10.1016/j.isci.2024.109720

Table 1. TARA cohort participant characteristics at entry

	HIV exposed infected	HIV exposed uninfected
Participants, *n*	43	46
Gender, M/F	17/26	24/22
Age, days (median, IQR)	34 (31–46)	32 (31–42)
VL log, cp/mL (median +/−SD)	5.9 ± 1.1	ND
CD4% <20% (n)	1	ND
[a]Mother VL, cp/mL (median +/− SD)	3.8 ± 1.5	ND
[a]Mother CD4, mm3 (median +/− SD)	357 ± 200	ND
Feeding practice, maternal/formula/combo (n)	35/3/5	39/2/5

[a]Result within 3 months after delivery.

RESULTS

89 infants born to mothers living with HIV were enrolled in a prospective, longitudinal cohort (TARA [Towards AIDS Remission Approaches]) in Mozambique (Table 1). 46 infants remained HIV negative and were followed up for 19 months. 43 infants were diagnosed with perinatally acquired HIV and initiated on ART at a median age of 34 days (Interquartile range (IQR), 31–46 days). Plasma virus load at study entry ranged from 312 to 10^7 HIV RNA copies/mL. 36 of HIV-infected children (HEI) completed 24 months of follow-up; 7 children left the study or died.[22] The incidence of viral suppression (VL < 200 copies/mL) was 23%, 44%, and 41% at 5, 10, and 18 months of age, respectively. Low viral suppression in the cohort was attributed to suboptimal ART adherence; however, 2 infants that never achieved viral suppression demonstrated resistance against 3TC and ABC at pre-ART.[22]

Rapid differentiation of CD8^{+} T cell compartment observed in perinatal HIV

To identify the early impact of HIV infection on T cell development in the TARA cohort, we analyzed T cell subset distribution and immunophenotype using high dimensional flow cytometry of cryopreserved peripheral blood mononuclear cells (PBMC) collected at pre-ART initiation from HEI and age-matched HEU infants (antibody panel listed in key resources table). In a subset of HEI and HEU, droplet microfluidic single-cell RNA sequencing (scRNA-seq) was also performed to define the transcriptional landscape of CD4 and CD8 T cells during early perinatal HIV infection (Figure 1A).

Evaluation of T cell frequencies and subset distribution revealed that frequencies of CD4^{+} T cells out of total CD3^{+} T cells were significantly reduced in HEI compared to HEU at entry (Figure 1B). However, the distribution of naive, memory, and effector cells within CD4^{+} T cells was largely similar in HEI and HEU infants, with the exception of transitional memory cells which were significantly reduced in HEI (median 2.2% in HEI vs. 3.8% in HEU). As expected naive cells (CD45RO− CD27^{+}) made up the majority of CD4^{+} T cells in 1–2 months old infants with a median of 86% at entry in both HEU and HEI. In addition to maturation subsets we also analyzed specialized CD4^{+} T cell subsets in infants including T regulatory (Treg) cells and peripheral T follicular helper (pTfh) cells in each group (Figure 1C). Treg cells represented 6.1% (IQR, 5.1–7.1) of CD4^{+} T cells in HEU at entry and comparison of Treg in HEU and HEI showed similar levels. pTfh cells were defined as CD4^{+} T central memory (TCM) expressing the GC homing chemokine receptor, CXCR5,[23] and did not exhibit significant differences between the groups. We analyzed an additional subset of Tfh, GC-like Tfh which were defined as PD-1+ CXCR5+ non-naive CD4^{+} T cells expressing high levels of CD38 and ICOS.[24] This population was very low in all infants (<0.05%) but was significantly higher in HEI at entry compared to HEU (Figure 1C).

Frequencies of CD8^{+} T cells out of total CD3^{+} T cells were not significantly different at entry between HEI and HEU (Figure 1D). Similar to CD4^{+} T cells in HEU, CD8^{+} T cells were predominantly naive phenotype (median 88%); however, in HEI CD8^{+} T cell subset distributions were skewed with significantly reduced naive frequencies (median 61%) and increased frequencies of TCM, T effector memory (TEM), and T effector (TE) suggesting viral induced maturation of the CD8^{+} T cell compartment in infants with perinatal HIV.

CD4^{+} and CD8^{+} T cells from HEI exhibit heighted activation at 1–2 months of age

To further characterize the infant T cell compartment, we measured single marker expression by flow cytometry on total CD4^{+} and CD8^{+} T cells and maturation subsets of 11 different surface markers related to cell homing/trafficking and immune activation and regulation including: CCR5, CCR7, CD25, CD28, CD31, CD38, CD127, HLA-DR, ICOS, PD-1, and TIGIT. We first characterized expression of each of the markers on T cells at 1–2 months of age in pre-ART HEI and HEU samples. Even at this early time point in immune development, all surface markers measured were detectable and showed anticipated expression patterns relative to T cell maturation state (i.e., higher frequency of activation marker expression on more differentiated cells and higher frequency of markers associated with self-renewal on less differentiated cells). Multiple markers of immune activation were elevated in CD8^{+} T cell subsets, including naive cells, in HEI compared to HEU such as HLA-DR, CD38, PD-1, and TIGIT (Figures 1E and S2). Markers associated with self-renewal and co-stimulation were reduced in HEI compared to HEU in multiple subsets including receptors: CD28, CD127, and CCR7. CD25, the high-affinity IL-2 receptor, was expressed at varying levels on memory CD8^{+} T cells (TCM and TEM) in HEU but was significantly reduced in HEI. CCR5 was highly expressed on memory and effector
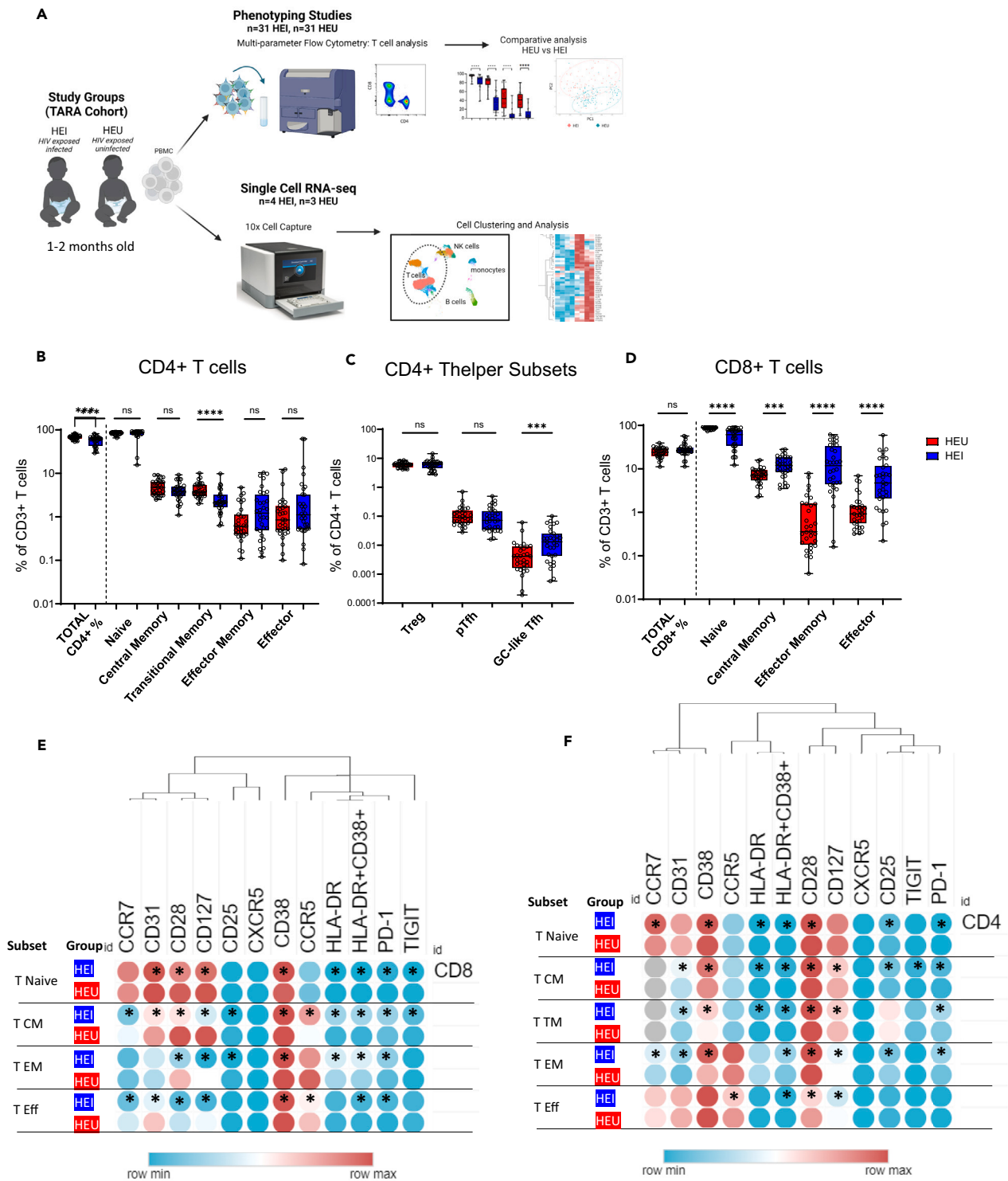
Figure 1. Impact of perinatal HIV on early T cell phenotypes

(A) Schematic of study design for evaluation of the T cell compartment in HIV-exposed infected and uninfected infants at 1–2 months of age.

(B) CD4$^+$ T cell frequencies are shown as frequencies of live CD3$^+$ lymphocytes and to the right of the dotted line CD4$^+$ T cell subsets are shown as frequencies out of total CD4$^+$ T cells for n = 31 HEU (red) and n = 32 HEI (blue).

(C) CD4$^+$ T cell helper subsets are shown as frequencies out of total CD4$^+$ T cells. Treg, T regulatory cells; pTfh, peripheral T follicular helper cells; GC, germinal center.

Figure 1. Continued

(D) CD8^{+} T cell frequencies are shown as frequencies of live CD3^{+} lymphocytes and to the right of the dotted line CD8^{+} T cell subsets are shown as frequencies of total CD8^{+} T cells. The gating strategy for defining cell populations is shown in Figure S1. Box and whisker plots show median and error bars represent the minimum and maximum values in each dataset. Mann-Whitney tests were performed for each subset between HEU and HEI and significance is shown using asterisks as follows *, $p < 0.05$; **, $p < 0.01$; ***, $p < 0.001$, and ****$p < 0.0001$.

(E and F) Heatmaps showing median expression of each cell surface receptor on CD8^{+} T cell subsets (E) and CD4^{+} T cell subsets (F). Hierarchical clustering was performed on columns to group markers with similar expression patterns. Mann-Whitney tests were performed for each marker expression between HEU and HEI and significance is shown using asterisks on the HEI data to represent a difference in expression in HEI relative to HEU (* = $p < 0.05$). Figures S2 and S3 show individual data points in box and whisker plots to understand directionality of changes in HEI relative to HEU.

CD8^{+} T cells in HEU and HEI but showed differences in TCM and Teff. Finally, CD31 (PECAM-1) a marker for transendothelial migration, was highly expressed on naive CD8^{+} T cells and intermediately on other subsets and showed significant reduction in HEI compared to HEU.

CD4^{+} T cell subsets from HEI exhibited higher expression of surface markers of activation including CD38, HLA-DR, and PD-1, as well as CD31 and CCR7 (Figures 1F and S3). Additionally, only in the TCM subset, ICOS and TIGIT expression were increased relative to HEU. Matching the observation in CD8^{+} T cells, CD127 and CD28 were reduced across multiple CD4^{+} T cell subsets in HEI. Interestingly, CCR5, the co-receptor for HIV entry, was not significantly different in expression on CD4^{+} T cell subsets except for Teff where it was reduced in HEI compared to HEU. CD25 expression was elevated in naive and TCM and reduced in TEM in HEI. These results demonstrate the broad phenotypic changes that the T cell compartment undergoes in the context of perinatal HIV infection leading to enrichment of mature and activated T cells.

Distinct CD8^{+} T cell cluster with cytolytic transcriptional profile identified in HEI at pre-ART

scRNA-seq was performed on PBMC from a subset of TARA HEI and HEU to assess transcriptional profiles associated with perinatal HIV infection compared to *in utero* exposure in the absence of acquisition. scRNA-seq experiments were run in parallel with flow cytometry data and selection was made based on matching age at sampling between HEI and HEU. All demographic characteristics for the 7 participants included in the scRNA-seq dataset are shown in Table 2. After integration and normalization of sequencing data, clusters were generated and manually annotated using top gene expression per cluster (Figures 2A and 2B). Clusters 0, 6, 11, and 14 represented CD3^{+} CD4^{+} T cells and clusters 2 and 3 represented CD3^{+} CD8^{+} T cells and thus were explored further for gene expression profiles.

Comparison of the cluster uniform manifold approximation and projection (UMAP) by separating HEI and HEU revealed that cluster 3 (CD8 cytotoxic T lymphocytes [CTL]-like) was present only in HEI and nearly absent in all 3 HEU donors (Figure 3A). Analysis of individual donor cell frequency per cluster showed that HEI exhibited decreased frequencies of cluster 2 (CD8 resting) with a median 16.4% in HEI vs. 20.8% in HEU, and increased frequencies of cluster 3 (CD8 CTL-like) with median of 8.1% in HEI vs. 0.1% in HEU (Figure 3B). Gene expression associated with cluster 2 is consistent with a naive, less differentiated cell state including expression of *CCR7*, *CD27*, *TCF7*, and *SELL* (Figure 2B). Cluster 3, on the other hand, exhibited low to no expression of these genes and instead expressed high levels of genes associated with cytolytic granules including *PRF1*, *GZMH*, *GZMB*, *NKG7*, and *GNLY* as well as other genes associated with CD8 effector function or regulation including *IFNG*, *FASLG*, *TIGIT*, *KLRC1*, *CCL3*, *CCL4*, and *PDCD1* relative to cluster 2 cells from HEI or HEU (Figure 3C). As observed in flow cytometry data, CD4^{+} T cell subsets show similar distributions in HEU and HEI with CD4 resting, Th2, and Treg cells making up 39%, 2.5%, and 1.9% of all cells in HEU and 41%, 2.4%, and 2% in HEI, respectively (Figure 3B). Based on gene expression profiling, the Th2 cluster showed highest expression of the chemokine receptor *CCR4*, compared to *CCR6* and *CXCR3* (Figure 3D). Treg were marked by high expression of *CTLA4*, *IL2RA*, *FOXP3*, and *TIGIT*. An additional Treg population was defined (cluster 6) as having high expression of the IL2R alpha chain (CD25) compared to Treg (cluster 14). This cluster was more abundant in HEU compared to HEI, however in both groups there were insufficient cells for further downstream analysis.

T cell receptor (TCR) clonotype analysis revealed that expansions observed in HEI in cluster C3 were oligoclonal populations that could be identified in each HEI participant (Figures 3E and 3D). Clonal expansion within other T cell subsets was not observed. Differential gene expression was assessed between HEI and HEU within T cell clusters with exception of CTL-like (cluster 3) due to inadequate cells available for analysis from HEU. For each comparison we observed over 600 genes that were differentially expressed; however, this number decreased when we applied an adjusted p value (<0.01) and fold change cutoff (>1.5) to visualize the genes with greatest change in expression (Figure S4). In CD4 resting cells HEI expressed higher levels of *HLA-C*, *ICAM2*, *IFITM1*, and *GZMA* and lower levels of *IL4R*, *BATF*, and *IRF1* which will likely alter the way these cells respond to stimuli *in vivo*. Th2 and Treg also showed upregulation of *HLA-C*, but CD8 resting cells did not, suggesting generalized upregulation of HLA-C expression in CD4 T cells.

Specific T cell phenotypes correlate with pre-ART virus load

Given the influence of HIV infection on T cells observed at pre-ART we assessed whether plasma virus load (VL) was directly related to the size (i.e., distribution) of a particular T cell subset in HEI from the TARA cohort. VL at study entry in HEI ranged across 5 logs raising the possibility that some degree of immune control could be occuring in infants with lower VL. We performed univariate correlation analysis of CD4^{+} and CD8^{+} T cell subsets from flow cytometry data with VL measurements (Figure 4). CD4^{+} T cell frequencies (out of total T cells) were not significantly associated with VL at this time point; however, specific T cell subsets exhibited associations with pre-ART VL. The strongest associations ($p < 0.01$) were observed between CD127 and CXCR5 expression on T cells. CD127 expression on multiple CD4^{+} T cell subsets including

Table 2. TARA Participants in scRNA-seq dataset

Group	ID	Sex	Weight (kg)	Age (days)[a]	Feeding practice	HIV cp/mL (log)	Days to VL < 400 cp/mL	Mother age (yrs)	Mother VL (c/mL)[b]	Mother CD4 (mm³)
HEU	CE021	F	3.6	31	AME					
HEU	CE025	F	4.3	35	AME					
HEU	CE037	M	4.9	33	AME					
HEI	CP002	F	3.8	30	AME	6.63	N/A	37	15786	550
HEI	CP003	M	3.4	32	AME	5.82	152	27	1552	1015
HEI	CP006	F	2.9	31	AME	7	93	34	500	535
HEI	CP018	F	3.5	35	AA	5.25	65	20	N/A	665

[a]Age at study entry and ART initiation; N/A, data not available.
[b]Result within 3 months after delivery.

naive, memory, and T helper populations was positively associated with VL. Negative correlations with pre-ART VL were observed with CXCR5-expressing CD4⁺ and CD8⁺ subsets with the frequency of GC-Tfh showing the strongest negative correlation with VL.

Effect of viral suppression on longitudinal T cell maturation

ART was initiated at HIV diagnosis in all TARA cohort infants; however, adherence was suboptimal during 18 months of follow-up. We assessed the impact of viral suppression on the distribution of maturation subsets longitudinally compared to HEU in the TARA cohort. Participants were divided into viremic or aviremic groups based on greater than or less than 200 HIV RNA copies/mL in plasma, respectively. CD4 frequencies were reduced in viremic compared to HEU at all longitudinal time points, while aviremic were not different than HEU except at 18 months (Figure 5A). A similar pattern was observed for CD4⁺ T cell maturation subsets where frequencies in aviremic, viremic, and HEU were not significantly different until the 18 months time point (Figures 5C–5E and 5G). CD8⁺ T cell frequencies were increased in viremic HEI in longitudinal time points leading to reduced CD4:CD8 ratios in viremic infants compared to aviremic and HEU (Figures 5B and S5). Evaluation of CD8⁺ T cell maturation subsets showed that aviremic HEI maintained altered distribution relative to HEU at 5 and 18 m post-ART with reduced naive and increased effector memory cells (Figures 5D, 5F, and 5H).

Distinct T cell parameters associate with age and HIV status in HIV exposed infants

To globally evaluate changes in the T cell compartment during immune development in the context of perinatal HIV infection we performed principal-component analysis (PCA) analysis using the entire longitudinal phenotypic dataset including single marker expression in total CD4⁺ and CD8⁺ T cells and maturation subsets. Samples from HEI and HEU clustered separately in PCA analysis along PC2 and this separation was observed at all time points (Figure 6A). Both groups migrated along the PC1 axis as age increased (Figure 6B). The top parameters that contributed to variation along PC1 were related to higher expression of markers related to self-renewal including CD28, CD127, and CCR7 in CD8⁺ T cells from pre-ART (Figure 6C). The parameters that were associated with increasing age were higher frequencies of total CD8⁺ T, CD8⁺ Teff, and TIGIT expression on CD4⁺ and CD8⁺ T cells. The top parameters contributing to variation along PC2 were related to immune activation with multiple CD4 and CD8 T cell subsets expressing HLA-DR or co-expression of HLA-DR and CD38 defining HEI samples as compared to HEU (Figure 6D). The parameters that were associated more closely with the HEU cluster was a higher frequency of CD127-expressing CD4⁺ TEM.

Finally, to understand direct effects of viral burden on T cell biology in infants, we performed correlation analyses with the top loadings for PC2 and VL (Table 3). The top parameter was CD8⁺ TCM HLA-DR+CD38⁺ cells, which strongly positively correlated with VL ($r = 0.59$, $p < 0.0001$). These data confirm that immune activation, determined by HLA-DR expression (with and without co-expression of CD38), of T cells is tightly associated with viral burden in infants.

DISCUSSION

The focus toward HIV cure strategies targeting children as well as adults has brought to the forefront the need to deeply characterize the infant immune system in the context of HIV exposure and infection.[9,11] Although it is recommended to start ART as early as possible in cases of perinatal HIV transmission, ART adherence leading to sustained viral suppression is challenging in newborns and young children.[1] The proportion of infants who were suppressed (<200 copies/mL) at 2 years in the TARA study cohort from Mozambique (43%) is similar to other early ART initiation cohorts from South Africa[25] and Cameroon.[26] The low adherence in the TARA cohort, however, provided an opportunity to explore the developing adaptive immune system in very young children in the context of HIV exposure (1) without HIV acquisition, (2) with HIV infection and ART-mediated viral suppression, and (3) with uncontrolled HIV infection. Here, we demonstrate that the CD8⁺ T cell compartment undergoes rapid maturation with transition of naive cells into terminally differentiated effector populations early after HIV acquisition. This effect on CD8⁺ T cells was observed during the neonatal period and longitudinally through 18 months of age in presence
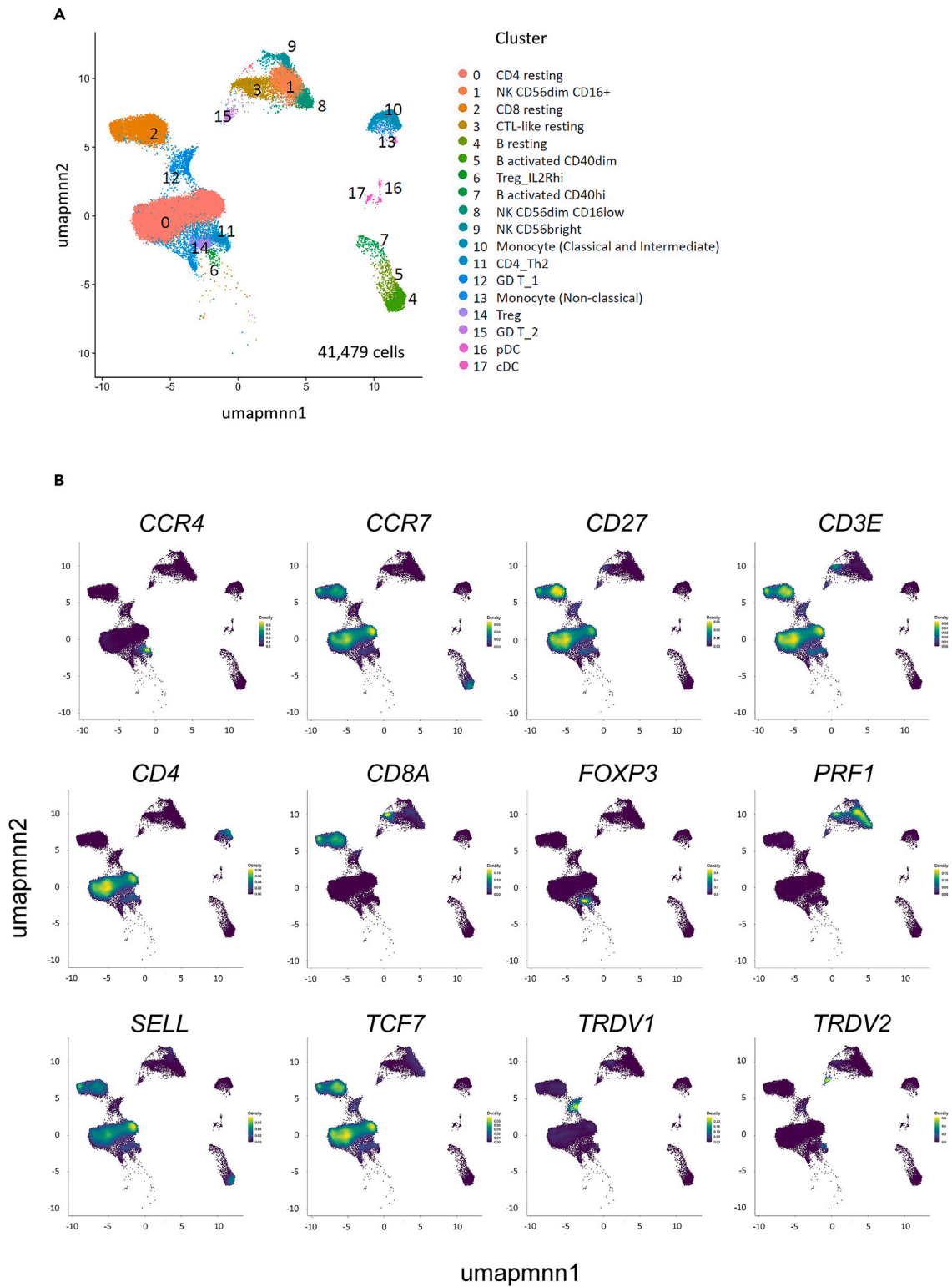
Figure 2. T cell clusters in scRNA-seq data from HEU and HEI at pre-ART, 1–2 months of age
(A) UMAP of PBMC cell clusters.
(B) Nebulosa plots showing indicated gene expression within clusters from the UMAP in (A).
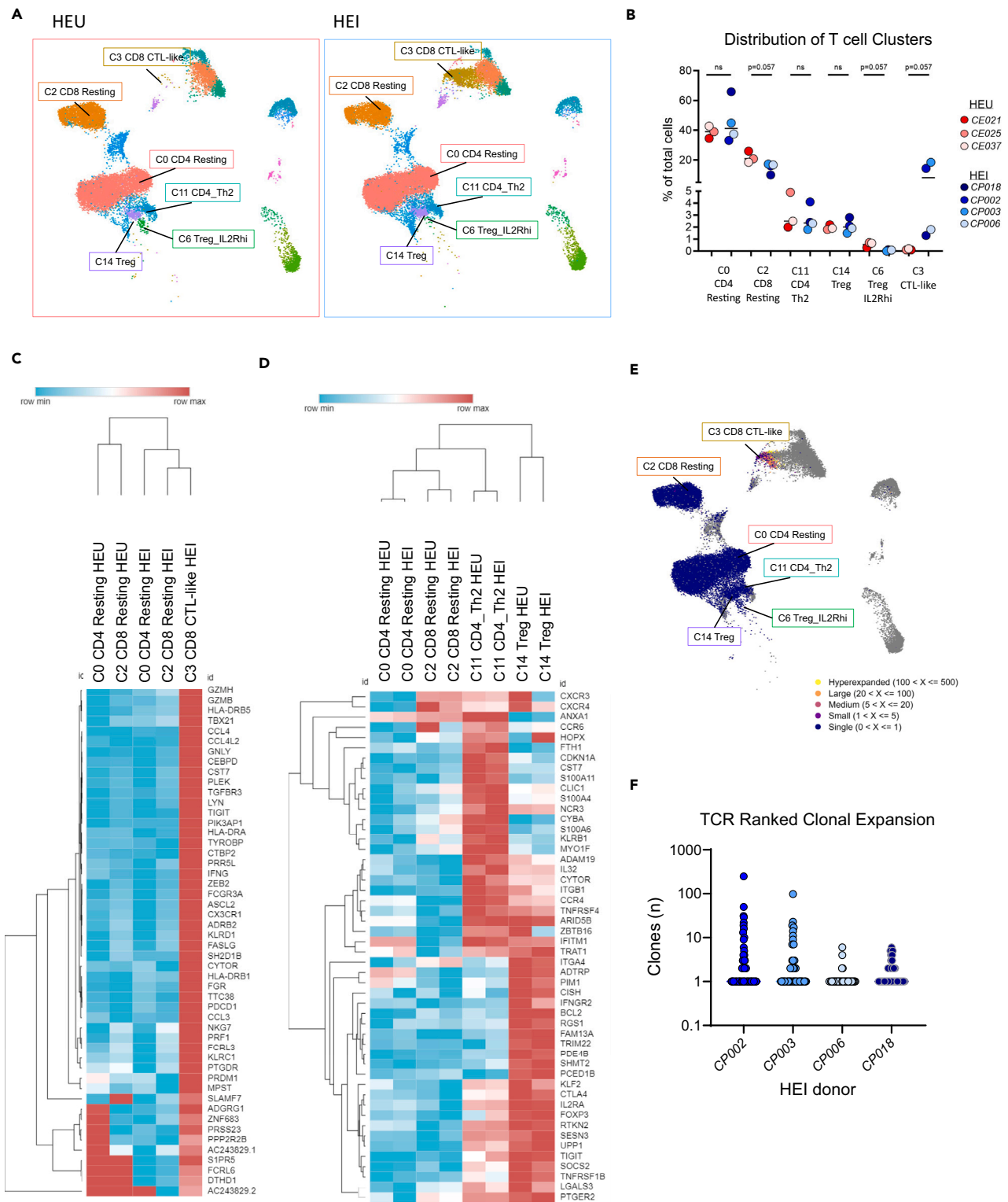
Figure 3. Identification of CD8^{+} CTL-like effector cell cluster in HEI

(A) UMAPS showing cells from HEU (left) and HEI (right) with labels of CD4^{+} and CD8^{+} T cell clusters.

(B) Distribution of each T cell cluster out of total cells by sample (individual donor). Mann-Whitney test was performed to compare frequencies from HEI donors
(*n* = 4) and HEU donors (*n* = 3).

Figure 3. *Continued*

(C) Top genes showing enrichment in C3 CD8 CTL-like cluster compared to C2 CD8 Resting cluster, also shown are C0 CD4 resting cluster gene expression for comparison.

(D) Top genes showing enrichment in C10 CD4 Th2 cluster and C13 CD4 Treg cluster relative to C0 CD4 resting cluster, also shown are C2 CD8 resting cluster for comparison.

(E) TCR clonotype analysis overlaid on UMAP of T cell clusters. Legend shows color-coding for size of expanded or unique clone.

(F) Quantification of clone size from each HEI participant.

and absence of viral suppression. scRNA-seq in a small subset of infants at pre-ART initiation supported findings from flow cytometry experiments and also revealed that enriched effector subsets represent a population of CD8^{+} CTL-like cells present only in HEI. Finally, our results highlight that the CD4^{+} T cell compartment is remarkably stable in maintaining age-appropriate distributions of distinct subsets, despite an overall reduction of CD4^{+} T cells during perinatal HIV infection.

We detected a robust adaptive immune response to HIV in 1-month-old infants. Although not directly tested in our system, we speculate that expanded CTL-like cells are HIV-specific since they were absent in HEU and we can also clearly rule out an artifact of HIV exposure *in utero*. CTLs are crucial for the control of HIV infection[27–30]; however, the CTL response is insufficient in most people to control infection due to viral escape, CD8^{+} T cell exhaustion, and exclusion of CD8^{+} T cells from reservoir sanctuary sites such as germinal centers of lymph nodes. Importantly, studies of natural HIV infection have demonstrated that HIV incurs a fitness cost when escaping from certain CTL responses, thus humans who target HIV through these epitopes show enhanced viral control (i.e., elite controllers).[31,32] The infant immune system is often characterized as immature or dysfunctional; however, emerging concepts point to unique transcriptional and epigenetic features of neonatal T cells that allow them to rapidly mount an effector response to infection.[33] In the context of perinatal HIV infection, specific CTL effector responses have been documented in children less than 1 year of age but these responses were not followed up longitudinally.

The frequency of CD8^{+} T cell effectors or degree of expansion within the unique CTL-like cluster did not show a significant association with plasma viremia in the TARA HEI. Studies in adults in the 1990s identified oligoclonal expansions in CD8^{+} T cells in acute HIV which were either cytotoxic or non-cytotoxic in response to HIV antigens and that waned over time.[34–36] Additionally, proliferation of CD8^{+} T cells in the blood lags behind the viral set point kinetics and these 2 metrics ware negatively correlated in acute infection suggesting a role in CTL expansion on shaping viral kinetics.[37] In the TARA cohort, the majority of infants were breastfed and were first tested for HIV at 1–2 months of age so exact timing of infection and viral set point could not be established.

The distribution of naive CD4^{+} T cell frequencies was in stark contrast to the distribution of naive CD8^{+} T cells observed in HEI. One explanation could be that CD8^{+} T cells have a faster rate of cell division than do CD4^{+} T cells and the amount of antigen exposure required to launch the differentiation program for naive CD8^{+} T cells is less than that required for naive CD4^{+} T cells. In fact, this difference was observed early at 1 to 2 months of age, with increases in activation markers in CD4^{+} and CD8^{+} T cells, and reduced expression of naive-cell markers in the HEI infants. The CD8^{+} T cell compartment exhibited striking differences in HEI compared to HEU with lower frequencies of naive CD8^{+} T cells at 1–2 months of age and memory cells with elevated expression of PD-1, TIGIT, CD38, HLA-DR, and CCR5 in HEI. Overall, our data support the strong relationship between virus load and immune activation, especially in the CD8^{+} T cell compartment, which has been shown in adults[38] and children,[39] and now even in 1–2 month old infants with perinatal HIV. In our cohort, naive cells represented 80–90% of cells in the CD4^{+} T cell compartment. Studies have shown that naive CD4^{+} T cells can be divided into two subsets based on CD31 (PECAM-1) expression.[40] CD31^{+} naive CD4 T cells represent thymic derived naive T cells while the loss of CD31 indicates peripheral proliferation has occurred (i.e., daughters of thymic emigrants). Our analysis showed that naive CD4^{+} T cells from HEI expressed higher amounts of CD31 compared to HEU reflective of increased thymic output of CD4^{+} T cells in HIV infected infants to replenish cells eliminated due to cytopathic effects of the virus. In line with previous work,[41] however, the distribution of CD31^{+} naive CD4 T cells in HEI did not show any relationship with virus load.

The factors that determine virus load in acute perinatal infection are likely to include a variety of infant and maternal factors including maternal virus load and pathogenic characteristics of the transmitted founder virus. In order to get a deeper understanding of the impact to the T cell compartment during acute HIV infection in infants we screened the dataset for T cell correlates of viral loads. Peripheral Tfh (pTfh and GC-like Tfh) stood out as interesting correlates given that T follicular helper cells (in lymph nodes and periphery) are known to harbor latent HIV.[42–46] The frequency of peripheral Tfh cells increased strongly with age in HEU and HEI infants. Previous studies have shown that neonates have very low levels of CXCR5 expression on CD4^{+} T cells which increase to adult levels by age 1.[47,48] In the TARA cohort, HEI and HEU had similar frequencies of pTfh (defined as CXCR5+ CD4^{+} central memory cells[23,49,50]) at 1–2 months of age; however, HEI had increased frequencies of the circulating GC-like Tfh which express ICOS and CD38 and have been shown in adults to increase in the periphery after vaccination or infection.[24,51] Tfh have been shown to be a sanctuary site for HIV reservoir during viremic and ART-treated HIV infection, so the relationship between CXCR5-expressing CD4 T cells and VL could reflect homing to lymph nodes out of the periphery or a direct effect whereby HIV-infected CD4^{+} CXCR5+ T cells are either eliminated or downregulate CXCR5 surface expression. Mechanistic studies will address whether the correlations observed reflect a direct or indirect relationship with HIV-infected cells or HIV-specific immune responses. HIV quantification was limited to plasma virus RNA measurements for correlations with immune phenotypes due to the small number of participants who exhibited sustained viral suppression. It is important to note that we made the assumption that viral suppression equals ART adherence based on clinical records and discussions with the mothers, however pediatric elite controllers and nonprogressors have been reported in ART naive individuals[12,52,53] and thus in the absence of drug testing in plasma samples we cannot completely rule out instances of ART-free viral control in this cohort.
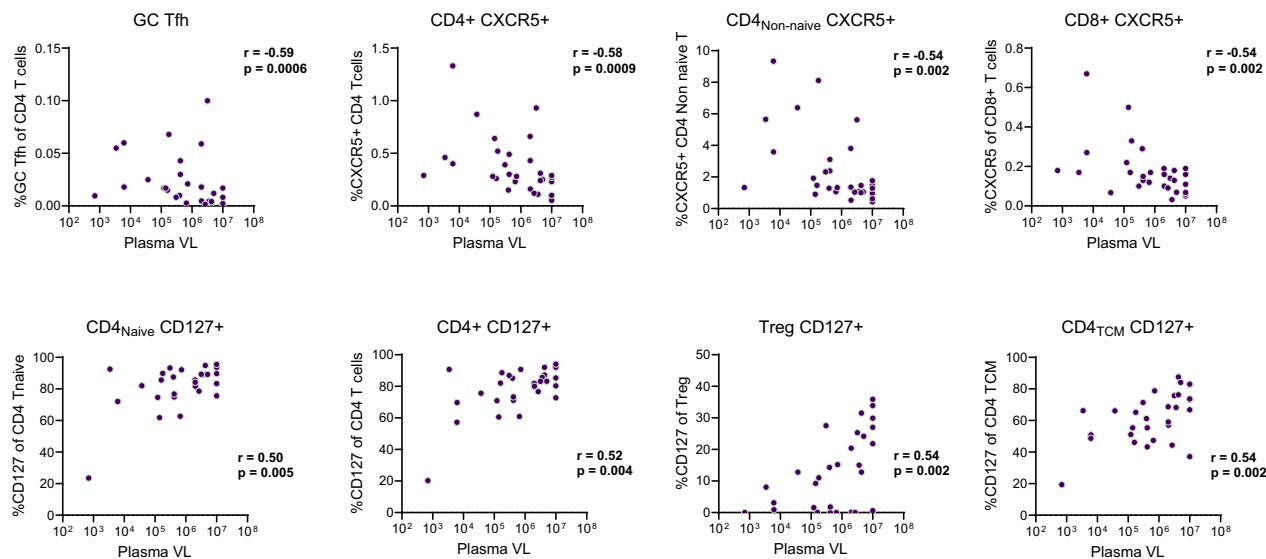
Figure 4. T cell phenotypes correlate with entry virus load

Spearman correlations were performed between infant plasma virus load and 320 T cell parameters measured at the same time point by flow cytometry in HEI ($n = 31$). Parameters that exhibited $p < 0.01$ are shown.

All T cell subsets from HEI exhibited reduced expression of the IL-7 receptor, CD127, compared to HEU at entry, suggesting increased circulating IL-7 in response to HIV infection. Downregulation of CD127 is associated with lower CD4 T cell counts and increased viral replication in adults and is implicated in reduced HIV specific CTL activity.[54,55] IL-7 is the major homeostatic cytokine supporting T cell survival. These results point to a unique role for IL7/IL7R signaling in early response to HIV infection in the neonatal period and suggest that magnitude of receptor downregulation on memory CD4 T cells, possibly in response to IL-7 levels, could be a correlate of viral control.

A limitation of the current study is that it only focused on T cells infant immune development is globally impacted during perinatal HIV infection, as we showed recently in an investigation of B cell and antibody responses to routine vaccines in the TARA cohort.[56] Additional studies are ongoing in the TARA cohort to examine the innate immune system as well. A strength of this cohort is the inclusion of HEU children as the comparator group for the impact of HIV infection on immune development. This group was advantageous because it controls for HIV exposure and also is easier to follow longitudinally as there is clinical benefit with frequent point-of-care HIV testing as a part of the follow up to identify seroconversion. A second limitation is the inability to include HIV unexposed uninfected infants that would have allowed us to examine immune development in the absence of HIV exposure. To our surprise, development of the T cell compartment, as shown by changes in phenotype in longitudinal samples, was in many ways consistent in HEI and HEU with a majority of the parameters assessed showing the same relationship with age (i.e., increase or decrease). However, the multivariable longitudinal analysis confirmed that increased immune activation is observed as early as 1–2 months of age and persists in the absence of ART throughout development. Overall, this study provides a resource for evaluation of T cell development in HIV exposed infants. We have identified T cell developmental changes directly attributable to HIV burden in HEI and provide a strategy for identifying age-independent correlates of viral control in infants that may be important to guide the design of immune-based interventions, including vaccines, in early life.

STAR★METHODS

Detailed methods are provided in the online version of this paper and include the following:

- KEY RESOURCES TABLE
- RESOURCE AVAILABILITY
  - Lead contact
  - Materials availability
  - Data and code availability
- EXPERIMENTAL MODEL AND STUDY PARTICIPANT DETAILS
- METHOD DETAILS
  - Sample collection and processing
  - Flow cytometry
  - Cell barcoding and single cell RNA sequencing (scRNA-Seq) library preparation
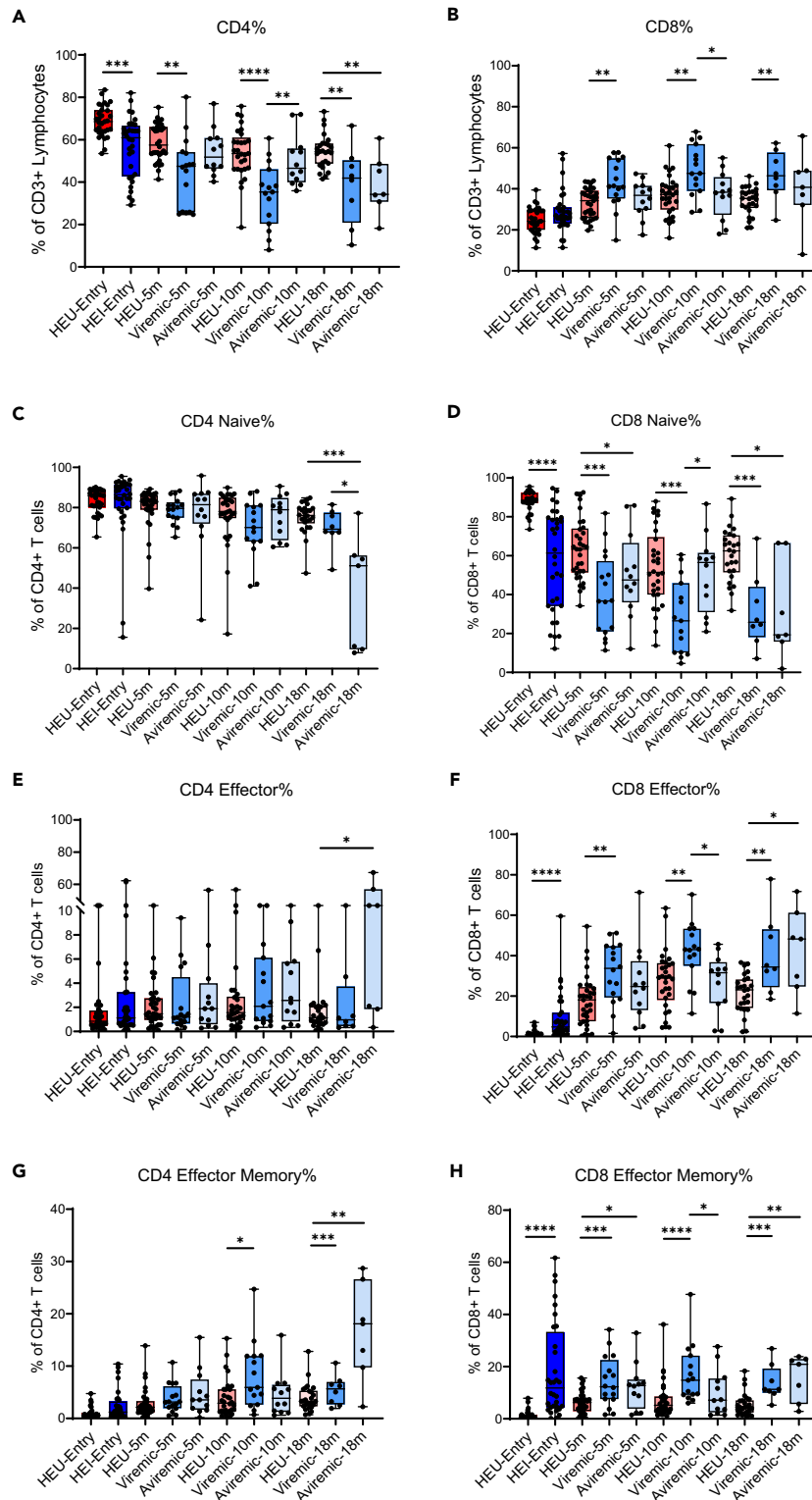
Figure 5. Impact of perinatal HIV on T cell differentiation in infants up to 18 months of age

(A and B) CD4+ (A) and CD8+ (B) T cell frequencies are shown as frequencies of live CD3+ lymphocytes for HEU (red) and HEI (blue).

(C, E, and G) CD4+ T cell helper subsets are shown as frequencies out of total CD4+ T cells.

Figure 5. *Continued*

(D, F, and H) CD8$^+$ T cell subsets are shown as frequencies of total CD8$^+$ T cells. Box and whisker plots show median and error bars represent the minimum and maximum values in each dataset. Number of samples in each dataset is as follows: HEI, entry (*n* = 32); aviremic, 5 months (*n* = 12), 10 months (*n* = 12), 18 months (*n* = 7); viremic, 5 months (*n* = 16), 10 months (*n* = 15), 18 months (*n* = 8); HEU, entry (*n* = 31), 5 months (*n* = 32), 10 months (*n* = 29), 18 months (*n* = 26). Mann-Whitney tests were performed for each subset between HEU and HEI and significance is shown using asterisks as follows *, *p* < 0.05; **, *p* < 0.01; ***, *p* < 0.001, and ****p < 0.0001.

- QUANTIFICATION AND STATISTICAL ANALYSIS
  - Flow cytometric data
  - scRNA-Seq data

SUPPLEMENTAL INFORMATION

Supplemental information can be found online at https://doi.org/10.1016/j.isci.2024.109720.
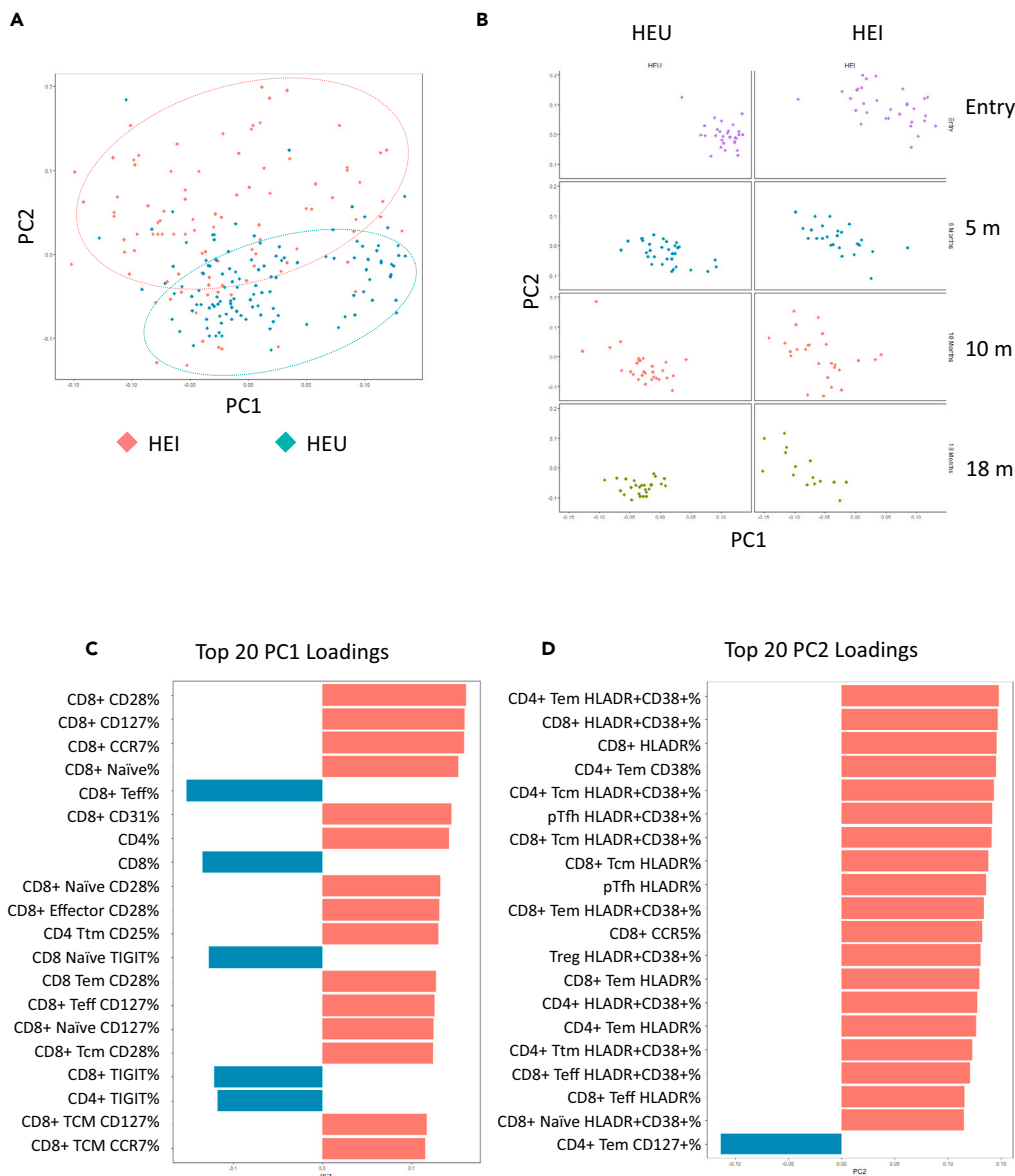
Figure 6. Longitudinal analysis of T cell phenotypes in HIV-exposed infants

(A and B) Multivariate PCA analyses show variation in T cell phenotypic profiles in relation to HIV status and time point in the groups.

(C and D) The PCA-selected features were also plotted and ranked in a VIP score plot for PC1 (C) and PC2 (D).

Table 3. Correlation of T cell parameters from PC2 loadings with plasma virus load in longitudinal TARA cohort

Parameter	r	95% confidence interval	p (two-tailed)
CD8+ TCM HLA-DR+CD38+%	0.5857	0.4316 to 0.7066	<0.0001
CD8+ TCM HLA-DR%	0.576	0.4195 to 0.6991	<0.0001
CD8+ HLA-DR+CD38+%	0.5015	0.3293 to 0.6414	<0.0001
CD8+ HLA-DR%	0.4891	0.3146 to 0.6316	<0.0001
CD8+ TEM HLA-DR+CD38+%	0.4653	0.2865 to 0.6127	<0.0001
CD8+ TEM HLA-DR+%	0.4608	0.2813 to 0.6092	<0.0001
CD8+ Teff HLA-DR+CD38+%	0.3914	0.2014 to 0.5530	<0.0001
CD4+ TEM HLA-DR+%	0.3763	0.1844 to 0.5406	0.0002
pTfh HLA-DR+%	0.3713	0.1787 to 0.5364	0.0002
CD8+ Teff HLA-DR+%	0.368	0.1751 to 0.5338	0.0002
CD4+ TEM HLA-DR+CD38+%	0.3468	0.1513 to 0.5161	0.0005
pTfh HLA-DR+CD38+%	0.3003	0.1002 to 0.4770	0.003
CD8+ CCR5+%	0.2524	0.04870 to 0.4360	0.0131
CD8+ naive HLA-DR+CD38+%	0.1812	−0.02598 to 0.3735	0.0772
CD4+ TTM HLA-DR+CD38+%	0.1547	−0.05330 to 0.3497	0.1325
CD4+ HLA-DR + CD38+%	−0.05756	−0.2607 to 0.1505	0.5775
CD4+ TCM HLA-DR+CD38+%	−0.06246	−0.2653 to 0.1457	0.5455
Treg HLA-DR+CD38+%	−0.1042	−0.3039 to 0.1043	0.3122
CD4+ TEM CD127+%	−0.1384	−0.3350 to 0.06988	0.1788

AUTHOR CONTRIBUTIONS

Conceptualization: L.R.d.A., V.D., S.Pallikkuth, S.R., N.C., R.P., P.P., M.G.L., and S.Pahwa. Investigation: L.R.d.A., V.D., S.Pallikkuth, S.R., and S.Pahwa. Project administration and supervision: P.P., P.V., M.G.L., and S.Pahwa. Data curation: L.R.d.A., V.D., A.I., S.R., and N.C. Formal analysis and visualization: L.R.d.A. and A.I. Funding acquisition: S.Pahwa. Writing – original draft preparation: L.R.d.A. and V.D.

DECLARATION OF INTERESTS

The authors declare no competing interests.

REFERENCES

1. Lain, M.G., Chicumbe, S., Cantarutti, A., Porcu, G., Cardoso, L., Cotugno, N., Palma, P., Pahwa, R., Pallikkuth, S., Rinaldi, S., et al. (2023). Caregivers' psychosocial assessment for identifying HIV-infected infants at risk of poor treatment adherence: an exploratory study in southern Mozambique. AIDS Care 35, 53–62. https://doi.org/10.1080/09540121.2022.2125159.

2. Brittain, K., Gomba, Y., Noholoza, S., Pellowski, J., Mellins, C.A., Bekker, L.G., Kagee, A., Remien, R.H., Abrams, E.J., and Myer, L. (2023). HIV-related stigma, disclosure and social support: experiences among young pregnant and postpartum women living with HIV in South Africa. AIDS Care 35, 399–405. https://doi.org/10.1080/09540121.2022.2121957.

3. Millar, J.R., Bengu, N., Fillis, R., Sprenger, K., Ntlantsana, V., Vieira, V.A., Khambati, N., Archary, M., Muenchhoff, M., Groll, A., et al. (2020). HIGH-FREQUENCY failure of combination antiretroviral therapy in

paediatric HIV infection is associated with unmet maternal needs causing maternal NON-ADHERENCE. EClinicalMedicine 22, 100344. https://doi.org/10.1016/j.eclinm.2020.100344.

4. IN DANGER: UNAIDS Global AIDS Update 2022 (2022 (Joint United Nations Programme on HIV/AIDS).

5. Payne, H., Chan, M.K., Watters, S.A., Otwombe, K., Hsiao, N.Y., Babiker, A., Violari, A., Cotton, M.F., Gibb, D.M., and Klein, N.J. (2021). Early ART-initiation and longer ART duration reduces HIV-1 proviral DNA levels in children from the CHER trial. AIDS Res. Ther. 18, 63. https://doi.org/10.1186/s12981-021-00389-1.

6. Foster, C., Domínguez-Rodríguez, S., Tagarro, A., Gkouleli, T., Heaney, J., Watters, S., Bamford, A., Fidler, K., Navarro, M., De Rossi, A., et al. (2021). The CARMA Study: Early Infant Antiretroviral Therapy-Timing Impacts on Total HIV-1 DNA Quantitation 12 Years Later. J. Pediatric Infect. Dis. Soc. 10, 295–301. https://doi.org/10.1093/jpids/piaa071.

7. Garcia-Broncano, P., Maddali, S., Einkauf, K.B., Jiang, C., Gao, C., Chevalier, J., Chowdhury, F.Z., Maswabi, K., Ajibola, G., Moyo, S., et al. (2019). Early antiretroviral therapy in neonates with HIV-1 infection restricts viral reservoir size and induces a distinct innate immune profile. Sci. Transl. Med. 11, eaax7350. https://doi.org/10.1126/scitranslmed.aax7350.

8. Persaud, D., Gay, H., Ziemniak, C., Chen, Y.H., Piatak, M., Jr., Chun, T.W., Strain, M., Richman, D., and Luzuriaga, K. (2013). Absence of detectable HIV-1 viremia after treatment cessation in an infant. N. Engl. J. Med. 369, 1828–1835. https://doi.org/10.1056/NEJMoa1302976.

9. Berendam, S.J., Nelson, A.N., Yagnik, B., Goswami, R., Styles, T.M., Neja, M.A., Phan, C.T., Dankwa, S., Byrd, A.U., Garrido, C., et al. (2022). Challenges and Opportunities of Therapies Targeting Early Life Immunity for Pediatric HIV Cure. Front. Immunol. 13, 885272. https://doi.org/10.3389/fimmu.2022.885272.

10. Martinez, D.R., Permar, S.R., and Fouda, G.G. (2016). Contrasting Adult and Infant Immune Responses to HIV Infection and Vaccination. Clin. Vaccine Immunol. 23, 84–94. https://doi.org/10.1128/CVI.00565-15.

11. Deeks, S.G., Archin, N., Cannon, P., Collins, S., Jones, R.B., de Jong, M.A.W.P., Lambotte, O., Lamplough, R., Ndung'u, T., Sugarman, J., et al. (2021). Research priorities for an HIV cure: International AIDS Society Global Scientific Strategy 2021. Nat. Med. 27, 2085–2098. https://doi.org/10.1038/s41591-021-01590-5.

12. Vieira, V., Lim, N., Singh, A., Leitman, E., Dsouza, R., Adland, E., Muenchhoff, M., Roider, J., Marin Lopez, M., Carabelli, J., et al. (2023). Slow progression of pediatric HIV associates with early CD8+ T cell PD-1 expression and a stem-like phenotype. JCI Insight 8, e156049. https://doi.org/10.1172/jci.insight.156049.

13. Olin, A., Henckel, E., Chen, Y., Lakshmikanth, T., Pou, C., Mikes, J., Gustafsson, A., Bernhardsson, A.K., Zhang, C., Bohlin, K., and Brodin, P. (2018). Stereotypic Immune System Development in Newborn Children. Cell 174, 1277–1292.e14. https://doi.org/10.1016/j.cell.2018.06.045.

14. Schatorjé, E.J.H., Gemen, E.F.A., Driessen, G.J.A., Leuvenink, J., van Hout, R.W.N.M., and de Vries, E. (2012). Paediatric reference values for the peripheral T cell compartment. Scand. J. Immunol. 75, 436–444. https://doi.org/10.1111/j.1365-3083.2012.02671.x.

15. Rackaityte, E., and Halkias, J. (2020). Mechanisms of Fetal T Cell Tolerance and Immune Regulation. Front. Immunol. 11, 588. https://doi.org/10.3389/fimmu.2020.00588.

16. Hayakawa, S., Ohno, N., Okada, S., and Kobayashi, M. (2017). Significant augmentation of regulatory T cell numbers occurs during the early neonatal period. Clin. Exp. Immunol. 190, 268–279. https://doi.org/10.1111/cei.13008.

17. Hartana, C.A., Garcia-Broncano, P., Rassadkina, Y., Lian, X., Jiang, C., Einkauf, K.B., Maswabi, K., Ajibola, G., Moyo, S., Mohammed, T., et al. (2022). Immune correlates of HIV-1 reservoir cell decline in early-treated infants. Cell Rep. 40, 111126. https://doi.org/10.1016/j.celrep.2022.111126.

18. Tsafaras, G.P., Ntontsi, P., and Xanthou, G. (2020). Advantages and Limitations of the Neonatal Immune System. Front. Pediatr. 8, 5. https://doi.org/10.3389/fped.2020.00005.

19. Levy, O. (2007). Innate immunity of the newborn: basic mechanisms and clinical correlates. Nat. Rev. Immunol. 7, 379–390. https://doi.org/10.1038/nri2075.

20. Huang, S., Dunkley-Thompson, J., Tang, Y., Macklin, E.A., Steel-Duncan, J., Singh-Minott, I., Ryland, E.G., Smikle, M., Walker, B.D., Christie, C.D.C., and Feeney, M.E. (2008). Deficiency of HIV-Gag-specific T cells in early childhood correlates with poor viral containment. J. Immunol. 181, 8103–8111. https://doi.org/10.4049/jimmunol.181.11.8103.

21. Klatt, N.R., Chomont, N., Douek, D.C., and Deeks, S.G. (2013). Immune activation and HIV persistence: implications for curative approaches to HIV infection. Immunol. Rev. 254, 326–342. https://doi.org/10.1111/imr.12065.

22. Lain, M.G., Vaz, P., Sanna, M., Ismael, N., Chicumbe, S., Simione, T.B., Cantarutti, A., Porcu, G., Rinaldi, S., de Armas, L., et al. (2022). Viral Response among Early Treated HIV Perinatally Infected Infants: Description of a Cohort in Southern Mozambique. Healthcare 10, 2156. https://doi.org/10.3390/healthcare10112156.

23. de Armas, L.R., Cotugno, N., Pallikkuth, S., Pan, L., Rinaldi, S., Sanchez, M.C., Gonzalez, L., Cagigi, A., Rossi, P., Palma, P., and Pahwa, S. (2017). Induction of IL21 in Peripheral T Follicular Helper Cells Is an Indicator of Influenza Vaccine Response in a Previously Vaccinated HIV-Infected Pediatric Cohort. J. Immunol. 198, 1995–2005. https://doi.org/10.4049/jimmunol.1601425.

24. Herati, R.S., Silva, L.V., Vella, L.A., Muselman, A., Alanio, C., Bengsch, B., Kurupati, R.K., Kannan, S., Manne, S., Kossenkov, A.V., et al. (2021). Vaccine-induced ICOS(+)CD38(+) circulating Tfh are sensitive biosensors of age-related changes in inflammatory pathways. Cell Rep. Med. 2, 100262. https://doi.org/10.1016/j.xcrm.2021.100262.

25. Veldsman, K.A., Laughton, B., Janse van Rensburg, A., Zuidewind, P., Dobbels, E., Barnabas, S., Fry, S., Cotton, M.F., and van Zyl, G.U. (2021). Viral suppression is associated with HIV-antibody level and HIV-1 DNA detectability in early treated children at 2 years of age. AIDS 35, 1247–1252. https://doi.org/10.1097/QAD.0000000000002861.

26. Ndongo, F.A., Tejiokem, M.C., Penda, C.I., Ndiang, S.T., Ndongo, J.A., Guemkam, G., Sofeu, C.L., Tagnouokam-Ngoupo, P.A., Kfutwah, A., Msellati, P., et al. (2021). Long-term outcomes of early initiated antiretroviral therapy in sub-Saharan children: a Cameroonian cohort study (ANRS-12140 Pediacam study, 2008-2013, Cameroon). BMC Pediatr. 21, 189. https://doi.org/10.1186/s12887-021-02664-6.

27. Betts, M.R., Nason, M.C., West, S.M., De Rosa, S.C., Migueles, S.A., Abraham, J., Lederman, M.M., Benito, J.M., Goepfert, P.A., Connors, M., et al. (2006). HIV nonprogressors preferentially maintain highly functional HIV-specific CD8+ T cells. Blood 107, 4781–4789. https://doi.org/10.1182/blood-2005-12-4818.

28. Turk, G., Ghiglione, Y., Falivene, J., Socias, M.E., Laufer, N., Coloccini, R.S., Rodriguez, A.M., Ruiz, M.J., Pando, M.Á., Giavedoni, L.D., et al. (2013). Early Gag immunodominance of the HIV-specific T-cell response during acute/early infection is associated with higher CD8+ T-cell antiviral activity and correlates with preservation of the CD4+ T-cell compartment. J. Virol. 87, 7445–7462. https://doi.org/10.1128/JVI.00865-13.

29. Borrow, P., Lewicki, H., Hahn, B.H., Shaw, G.M., and Oldstone, M.B. (1994). Virus-specific CD8+ cytotoxic T-lymphocyte activity associated with control of viremia in primary human immunodeficiency virus type 1 infection. J. Virol. 68, 6103–6110. https://doi.org/10.1128/JVI.68.9.6103-6110.1994.

30. Jones, R.B., and Walker, B.D. (2016). HIV-specific CD8(+) T cells and HIV eradication. J. Clin. Invest. 126, 455–463. https://doi.org/10.1172/JCI80566.

31. Rutishauser, R.L., and Trautmann, L. (2022). CD8 + T-cell responses in HIV controllers: potential implications for novel HIV remission strategies. Curr. Opin. HIV AIDS 17, 315–324. https://doi.org/10.1097/COH.0000000000000748.

32. Hartana, C.A., and Yu, X.G. (2021). Immunological effector mechanisms in HIV-1 elite controllers. Curr. Opin. HIV AIDS 16, 243–248. https://doi.org/10.1097/COH.0000000000000693.

33. Smith, N.L., Patel, R.K., Reynaldi, A., Grenier, J.K., Wang, J., Watson, N.B., Nzingha, K., Yee Mon, K.J., Peng, S.A., Grimson, A., et al. (2018). Developmental Origin Governs CD8(+) T Cell Fate Decisions during Infection. Cell 174, 117–130.e14. https://doi.org/10.1016/j.cell.2018.05.029.

34. Pantaleo, G., Demarest, J.F., Soudeyns, H., Graziosi, C., Denis, F., Adelsberger, J.W., Borrow, P., Saag, M.S., Shaw, G.M., Sekaly, R.P., et al. (1994). Major expansion of CD8+ T cells with a predominant V beta usage during the primary immune response to HIV. Nature 370, 463–467. https://doi.org/10.1038/370463a0.

35. Toso, J.F., Chen, C.H., Mohr, J.R., Piglia, L., Oei, C., Ferrari, G., Greenberg, M.L., and Weinhold, K.J. (1995). Oligoclonal CD8 lymphocytes from persons with asymptomatic human immunodeficiency virus (HIV) type 1 infection inhibit HIV-1 replication. J. Infect. Dis. 172, 964–973. https://doi.org/10.1093/infdis/172.4.964.

36. Weekes, M.P., Wills, M.R., Mynard, K., Hicks, R., Sissons, J.G., and Carmichael, A.J. (1999). Large clonal expansions of human virus-specific memory cytotoxic T lymphocytes within the CD57+ CD28- CD8+ T-cell

population. Immunology *98*, 443–449. https://doi.org/10.1046/j.1365-2567.1999.00901.x.

37. Ndhlovu, Z.M., Kamya, P., Mewalal, N., Kløverpris, H.N., Nkosi, T., Pretorius, K., Laher, F., Ogunshola, F., Chopera, D., Shekhar, K., et al. (2015). Magnitude and Kinetics of CD8+ T Cell Activation during Hyperacute HIV Infection Impact Viral Set Point. Immunity *43*, 591–604. https://doi.org/10.1016/j.immuni.2015.08.012.

38. Sangwan, J., Sen, S., Gupta, R.M., Shanmuganandan, K., and Grewal, R.S. (2020). Immune activation markers in individuals with HIV-1 disease and their correlation with HIV-1 RNA levels in individuals on antiretroviral therapy. Med. J. Armed Forces India *76*, 402–409. https://doi.org/10.1016/j.mjafi.2019.06.005.

39. Pereira-Manfro, W.F., Silva, G.P.D., Costa, P.R., Costa, D.A., Ferreira, B.D.S., Barreto, D.M., Frota, A.C.C., Hofer, C.B., Kallas, E.G., and Milagres, L.G. (2023). Expression of TIGIT, PD-1 and HLA-DR/CD38 markers on CD8-T cells of children and adolescents infected with HIV and uninfected controls. Rev. Inst. Med. Trop. Sao Paulo *65*, e14. https://doi.org/10.1590/S1678-9946202365014.

40. Kohler, S., and Thiel, A. (2009). Life after the thymus: CD31+ and CD31- human naive CD4+ T-cell subsets. Blood *113*, 769–774. https://doi.org/10.1182/blood-2008-02-139154.

41. Wightman, F., Solomon, A., Khoury, G., Green, J.A., Gray, L., Gorry, P.R., Ho, Y.S., Saksena, N.K., Hoy, J., Crowe, S.M., et al. (2010). Both CD31(+) and CD31(-) naive CD4(+) T cells are persistent HIV type 1-infected reservoirs in individuals receiving antiretroviral therapy. J. Infect. Dis. *202*, 1738–1748. https://doi.org/10.1086/656721.

42. Perreau, M., Savoye, A.L., De Crignis, E., Corpataux, J.M., Cubas, R., Haddad, E.K., De Leval, L., Graziosi, C., and Pantaleo, G. (2013). Follicular helper T cells serve as the major CD4 T cell compartment for HIV-1 infection, replication, and production. J. Exp. Med. *210*, 143–156. https://doi.org/10.1084/jem.20121932.

43. Fukazawa, Y., Park, H., Cameron, M.J., Lefebvre, F., Lum, R., Coombes, N., Mahyari, E., Hagen, S.I., Bae, J.Y., Reyes, M.D., 3rd, et al. (2012). Lymph node T cell responses predict the efficacy of live attenuated SIV vaccines. Nat. Med. *18*, 1673–1681. https://doi.org/10.1038/nm.2934.

44. Pallikkuth, S., Sharkey, M., Babic, D.Z., Gupta, S., Stone, G.W., Fischl, M.A., Stevenson, M., and Pahwa, S. (2015). Peripheral T Follicular Helper Cells Are the Major HIV Reservoir within Central Memory CD4 T Cells in Peripheral Blood from Chronically HIV-Infected Individuals on Combination Antiretroviral Therapy. J. Virol. *90*, 2718–2728. https://doi.org/10.1128/JVI.02883-15.

45. Fromentin, R., Bakeman, W., Lawani, M.B., Khoury, G., Hartogensis, W., DaFonseca, S., Killian, M., Epling, L., Hoh, R., Sinclair, E., et al. (2016). CD4+ T Cells Expressing PD-1, TIGIT and LAG-3 Contribute to HIV Persistence during ART. PLoS Pathog. *12*, e1005761. https://doi.org/10.1371/journal.ppat.1005761.

46. Rinaldi, S., de Armas, L., Dominguez-Rodríguez, S., Pallikkuth, S., Dinh, V., Pan, L., Gärtner, K., Pahwa, R., Cotugno, N., Rojo, P., et al. (2021). T cell immune discriminants of HIV reservoir size in a pediatric cohort of perinatally infected individuals. PLoS Pathog. *17*, e1009533. https://doi.org/10.1371/journal.ppat.1009533.

47. Shalekoff, S., Loubser, S., Dias, B.D.C., Strehlau, R., Shiau, S., Wang, S., He, Y., Abrams, E.J., Kuhn, L., and Tiemessen, C.T. (2021). Normalization of B Cell Subsets but Not T Follicular Helper Phenotypes in Infants With Very Early Antiretroviral Treatment. Front. Pediatr. *9*, 618191. https://doi.org/10.3389/fped.2021.618191.

48. Juno, J.A., and Hill, D.L. (2022). T follicular helper cells and their impact on humoral responses during pathogen and vaccine challenge. Curr. Opin. Immunol. *74*, 112–117. https://doi.org/10.1016/j.coi.2021.11.004.

49. Pallikkuth, S., Parmigiani, A., Silva, S.Y., George, V.K., Fischl, M., Pahwa, R., and Pahwa, S. (2012). Impaired peripheral blood T-follicular helper cell function in HIV-infected nonresponders to the 2009 H1N1/09 vaccine. Blood *120*, 985–993. https://doi.org/10.1182/blood-2011-12-396648.

50. Pallikkuth, S., de Armas, L.R., Rinaldi, S., George, V.K., Pan, L., Arheart, K.L., Pahwa, R., and Pahwa, S. (2019). Dysfunctional peripheral T follicular helper cells dominate in people with impaired influenza vaccine responses: Results from the FLORAH study. PLoS Biol. *17*, e3000257. https://doi.org/10.1371/journal.pbio.3000257.

51. Herati, R.S., Reuter, M.A., Dolfi, D.V., Mansfield, K.D., Aung, H., Badwan, O.Z., Kurupati, R.K., Kannan, S., Ertl, H., Schmader, K.E., et al. (2014). Circulating CXCR5+PD-1+ response predicts influenza vaccine antibody responses in young adults but not elderly adults. J. Immunol. *193*, 3528–3537. https://doi.org/10.4049/jimmunol.1302503.

52. Vieira, V.A., Millar, J., Adland, E., Muenchhoff, M., Roider, J., Guash, C.F., Peluso, D., Thomé, B., Garcia-Guerrero, M.C., Puertas, M.C., et al. (2022). Robust HIV-specific CD4+ and CD8+ T-cell responses distinguish elite control in adolescents living with HIV from viremic nonprogressors. AIDS *36*, 95–105. https://doi.org/10.1097/QAD.0000000000003078.

53. Ofori-Mante, J.A., Kaul, A., Rigaud, M., Fidelia, A., Rochford, G., Krasinski, K., Chandwani, S., and Borkowsky, W. (2007). Natural history of HIV infected pediatric long-term or slow progressor population after the first decade of life. Pediatr. Infect. Dis. J. *26*, 217–220. https://doi.org/10.1097/01.inf.0000254413.11246.e1.

54. Crawley, A.M., and Angel, J.B. (2012). The influence of HIV on CD127 expression and its potential implications for IL-7 therapy. Semin. Immunol. *24*, 231–240. https://doi.org/10.1016/j.smim.2012.02.006.

55. Sharma, T.S., Hughes, J., Murillo, A., Riley, J., Soares, A., Little, F., Mitchell, C.D., and Hanekom, W.A. (2008). CD8+ T-cell interleukin-7 receptor alpha expression as a potential indicator of disease status in HIV-infected children. PLoS One *3*, e3986. https://doi.org/10.1371/journal.pone.0003986.

56. Cotugno, N., Pallikkuth, S., Sanna, M., Dinh, V., de Armas, L., Rinaldi, S., Davis, S., Linardos, G., Pascucci, G.R., Pahwa, R., et al. (2023). B-cell immunity and vaccine induced antibody protection reveal the inefficacy of current vaccination schedule in infants with perinatal HIV-infection in Mozambique, Africa. EBioMedicine *93*, 104666. https://doi.org/10.1016/j.ebiom.2023.104666.

57. Hao, Y., Hao, S., Andersen-Nissen, E., Mauck, W.M., 3rd, Zheng, S., Butler, A., Lee, M.J., Wilk, A.J., Darby, C., Zager, M., et al. (2021). Integrated analysis of multimodal single-cell data. Cell *184*, 3573–3587.e29. https://doi.org/10.1016/j.cell.2021.04.048.

58. Zhang, F., Wu, Y., and Tian, W. (2019). A novel approach to remove the batch effect of single-cell data. Cell Discov. *5*, 46. https://doi.org/10.1038/s41421-019-0114-x.

59. Borcherding, N., Bormann, N.L., and Kraus, G. (2020). scRepertoire: An R-based toolkit for single-cell immune receptor analysis. F1000Res. *9*, 47. https://doi.org/10.12688/f1000research.22139.2.

60. Wu, T., Hu, E., Xu, S., Chen, M., Guo, P., Dai, Z., Feng, T., Zhou, L., Tang, W., Zhan, L., et al. (2021). clusterProfiler 4.0: A universal enrichment tool for interpreting omics data. Innovation *2*, 100141. https://doi.org/10.1016/j.xinn.2021.100141.

STAR★METHODS

KEY RESOURCES TABLE

REAGENT or RESOURCE	SOURCE	IDENTIFIER
Antibodies		
eBioscience AlexaFluor 532 mouse anti-human CD45 Antibody (clone HI30)	ThermoFisher	Cat# 58-0459-42, RRID:AB_11218673
BD Horizon BUV496 mouse anti-human CD4 Antibody (clone SK3)	BD	Cat# 612936, RRID:AB_2870220
BD Horizon BV710 mouse anti-human CD3 Antibody (clone UCHT1)	BD	Cat# 563109, RRID:AB_2732053
BD Pharmingen PerCP-Cy5.5 mouse anti-human CD8 Antibody (clone SK1)	BD	Cat# 565310, RRID:AB_2687497
eBioscience eFluor450 mouse anti-human CD27 Antibody (clone O323)	ThermoFisher	Cat# 48-0279-42, RRID:AB_10852844
BD Horizon BV563 mouse anti-human CD25 Antibody (clone 2A3)	BD	Cat# 612918, RRIB:AB_2870203
BD Horizon BV650 mouse anti-human CD45RO Antibody (clone UCHL1)	BD	Cat# 563750, RRID: AB_2744412
PerCP-eFluor710 rat anti-human CD197 (CCR7) Antibody (clone 3D12)	ThermoFisher	Cat# 46-1979-42, RRID:AB_10853814
BD Horizon BUV737 mouse anti-human CD127 Antibody (clone HIL-7R-M21)	BD Biosciences	Cat# 612794, RRID:AB_2870121
BD Horizon BV480 mouse anti-human CD38 Antibody (clone HIT2)	BD	Cat# 566137, RRID:AB_2739535
BV785 mouse anti-human CD28 Antibody (clone CD28.2)	Biolegend	Cat# 302950, RRID:AB_2632607
BD Horizon BUV661 mouse anti-human HLA-DR (clone G46-6)	BD	Cat# 612980, RRID:AB_2870252
AlexaFluor 647 anti-human TIGIT Antibody (clone A15153G)	Biolegend	Cat# 372724, RRID:AB_2715971
APC anti-human CD279 (PD-1) Antibody (clone EH12.2H7)	Biolegend	Cat# 329908, RRID:AB_940475
BD Horizon BB700 mouse anti-human CD31 Antibody (clone WM59)	BD	Cat# 566563, RRID:AB_2744362
BD Horizon BV421 rat anti-human CXCR5 Antibody (clone RF8B2)	BD	Cat# 562747, RRID:AB_2737766
PE/Cyanine7 anti-human/mouse/rat CD278 (ICOS) Antibody (clone C398.4A)	Biolegend	Cat# 313520, RRID:AB_10641839
PE rat anti-human CD195 (CCR5) Antibody (clone J418F1)	Biolegend	Cat# 359106, RRID:AB_2562334
Human Trustain FcX	Biolegend	Cat# 422302, RRID:AB_2818986
Chemicals, peptides, and recombinant proteins		
LIVE/DEAD™ Fixable Aqua Dead Cell Stain Kit	Thermo-Fisher	L34966
Critical commercial assays		
COBAS Ampliprep/Taqman HIV-1 Test	Roche Diagnostics	Version 2.0
Immune Profiling V2	10x Genomics	1000263, 1000286, 1000250, 1000215, 1000252,1000253, 1000190, 1000541
Viastain AO/PI	Nexelcom	CS2-0106
Deposited data		
Single Cell RNA sequencing BAM files and raw and normalized counts	Gene expression Omnibus	GSE254645
Software and algorithms		
Spectroflow Software	Cytek	Version 2.2.0.4
FlowJo Software	BD	Version 10.8.1
Basespace Software	Ilumina	Version 7.8
Cellometer k2	Nexelcom	
Cell Ranger Software	10x Genomics	Version 6
Prism Software	GraphPad	Version 9.1.2

RESOURCE AVAILABILITY

Lead contact

Further information and requests for resources and reagents should be directed to and will be fulfilled by the lead contact, Savita Pahwa (spahwa@med.miami.edu).

Materials availability

This study did not generate new unique reagents.

Data and code availability

- Single cell RNA-seq data have been deposited at GenBank and are publicly available as of the date of publication. Accession numbers are listed in the key resources table.
- This paper does not report original code.
- Any additional information required to reanalyze the data reported in this paper is available from the lead contact upon request.

EXPERIMENTAL MODEL AND STUDY PARTICIPANT DETAILS

Towards AIDS Remission Approaches (TARA) Cohort.Infants born to women living with HIV were recruited at the Machava and Matola Health Centers in Maputo Province, Mozambique.[1] For establishing HIV status, PCR testing was performed on blood samples using point of care technology, Alere™ q HIV-1/2 molecular diagnostic platform. Infants with 2 consecutive positive PCR tests were diagnosed as HIV exposed infected (HEI), and those with 2 negative PCR tests were diagnosed as HIV exposed uninfected (HEU). Infants were enrolled at 1-2 months of age with signed informed consent from the legal caregiver. All HIV exposed infants were given post-natal HIV prophylaxis with Nevirapine, which was disccontinued at age 6 weeks in HEU. In the HEI, triple drug ART was initiated with zidovudine (AZT) or Abacavir (ABC), Lamivudine (3TC) and Lopinavir/Ritonavir (LPV/rit). All infants received routine vaccinations as designated by local recommendations including BCG, DTaP-HepB-Hib-PCV10-OP at 2, 3 and 4 months of age and measles-rubella vaccine at 9 and 18 months of age. The study was approved by the National Bioethical Committee (102/CNBS/2016), the Mozambican Ministry of Health and Institutional review board at the University of Miami (IRB #20160493). The protocol was designed to enroll 45 HEU and 45 HEI to follow up for 24 months.

METHOD DETAILS

Sample collection and processing

Peripheral blood was collected in EDTA tubes at multiple timepoints throughout the study before and after starting ART. HIV-1 Plasma viral load (VL) was quantified using COBAS® AmpliPrep/COBAS® TaqMan® HIV-1 Test, version 2.0 (Roche Diagnostics, Germany) with a limit of detection of 20 copies/ml at the following intervals: 1, 2, 4, 5, 8, 9,11, 17, 17 and 1 week, 18 and 23 months after ART initiation. For additional immunologic and virologic assays, blood was processed at the Molecular Virology and Immunology laboratory of the National Institute of Health in Maputo. Peripheral blood mononuclear cells (PBMC) and plasma were cryopreserved onsite until shipment from Mozambique to University of Miami, FL in liquid nitrogen cryoshippers or dry ice, respectively.

Flow cytometry

Cryopreserved PBMC were thawed and rested overnight in complete medium (RPMI-1640 media containing L-glutamine, Pen-strep, and 10% Fetal Bovine Serum (FBS)) at 37°C and 5% CO2. 1 to 1.5 million PBMC were blocked with Human TruStain FcX (Biolegend) before being labeled with monoclonal antibodies. For T cell specific immunophenotyping, the panel included 19 fluorochrome-conjugated antibodies and a viability dye. All reagents were tested and titrated for optimum concentration before usage. Labeled PBMC were fixed in 1% paraformaldehyde (PFA) before acquisition on the Cytek Aurora Flow Cytometer. Compensation beads were used to create the single-color controls and prepared in the exact same manner as labeled PBMC. Single-color bead controls and unstained cells were used in the SpectroFlo software (version 2.2.0.4) for spectral unmixing and autofluorescence extraction. After sample acquisition, unmixed Flow Cytometry Standard (FCS) files were exported for analysis in FlowJo (version 10.8.1). Manual gating of T cell populations and markers were performed before being exported for further analysis.

Cell barcoding and single cell RNA sequencing (scRNA-Seq) library preparation

Cell suspensions were analyzed with a Nexcelom K2 digital cell counter to determine viability (AO-PI fluorescence) and total particles (bright field). Samples with viabilities from 69.2% (min) - 83.6 (average) - 93.3 (max) and concordant fluorescent and brightfield cell counts were captured using a 10X Genomics Chromium single cell controller with Immune Profiling V2 chemistry to target 8,000 - 10,000 cells. Post processing yields were 3,188 – 7,108 cells (Table S1). cDNA amplification and library preparation for gene expression profiling and V(D)J sequencing were carried out according to manufacturer's instructions without modification (10x Genomics PN: 1000263, 1000286, 1000250, 1000215, 1000252,1000253, 1000190, 1000541). Libraries were sequenced on an Illumina NovaSeq 6000 following 10X Genomics sequencing parameters. The resulting intensity files were demultiplexed as FASTQ files using Illumina BaseSpace software with subsequent alignment and counting using the 10x Genomics Cell Ranger V6 software package. All libraries generated summary performance metrics/data QC within 10X Genomics thresholds. BAM files and raw and normalized counts for all single-cell RNA sequencing data presented in this article have been submitted to Gene Expression Omnibus (GEO: https://www.ncbi.nlm.nih.gov/geo/query/acc.cgi?acc=GSE254645https://www.ncbi.nlm.nih.gov/geo/query/acc.cgi?acc=GSE).

QUANTIFICATION AND STATISTICAL ANALYSIS

Flow cytometric data

Comparisons between 2 groups for flow cytometry data were made using unpaired t test or Mann-Whitney u test, depending on normality of individual datasets. Correlations of T cell phenotypic data with HIV viral load was evaluated using Spearman test. Statistical tests were considered statistically significant with a p value ≤0.05 and performed using GraphPad Prism version 9.1.2 for Windows. Heatmaps were generated using Morpheus (https://software.broadinstitute.org/morpheus). The Non-linear Partial Least Squares (NIPALS) Algorithm was used to scale and center flow cytometry data, impute missings, and perform PCA using the nipals package in R. The preprocessing procedures included combining longitudinal T cell subset frequencies at 1-2 months, 5 months, 10 months, 18 months from HEI and HEU.

scRNA-Seq data

Bioinformatic analysis began with mapping and alignment to the human reference genome performed with Cell Ranger (10X Genomics), followed by rigorous quality control to remove droplets, doublets, and dead cells. After the Cell Ranger pipeline, subsequent analysis was performed using R. The different samples were then normalized and integrated using Seurat[57] Fastmnn,[58] respectively, to achieve cross-sample clustering and comparison. Resulting clusters were visualized using Uniform Manifold Approximation and Projection (UMAP) plots and were manually annotated based on gene expression of lineage markers to define cell populations and V(D)J analysis was performed using the R package scRepertoire.[59] Differential Expression was used to study the differences in clusters in HEI and HEU, and was performed using Wilcoxin's test, with adjusted p-values generated using Bonferroni Correction. Finally, pathway analysis was performed over various databases such as the Molecular Signatures Database (MSigDB), Kyoto Encyclopedia of Genes and Genomes (KEGG), and Reactome, using Gene Set Enrichment Analysis (GSEA) and Gene Ontology (GO) based approaches.[60]